Broadband Conductor Backed-CPW with Tapered Microstrip Line to Corrugated Via Wall-SIW Transition for Different-Bands (2-40 GHz)

Anil Kumar Nayak†‡, Igor M Filanovsky†, Kambiz Moez†, Amalendu Patnaik‡,
iCAS Laboratory† *Advanced Microwave Laboratory*‡
Dept. of Electrical and Computer Engg.† *Dept. of Electronics and Communication Engg.*‡
University of Alberta† *Indian Institute of Technology Roorkee*‡
Alberta, Canada Roorkee, India
Email: aknayak@ualberta.ca; ifilanov@ualberta.ca; kambiz@ualberta.ca; amalendu.patnaik@ece.iitr.ac.in

2023 IEEE International Symposium on Circuits and Systems (ISCAS) | 978-1-6654-5109-3/23/$31.00 ©2023 IEEE | DOI: 10.1109/ISCAS46773.2023.10181554

***Abstract*—This paper proposes the Corrugated Via-Wall Substrate Integrated Waveguide (CVWSIW) (with enhanced performance compared to the traditional SIW) and the transitions to this newly proposed CVWSIW from a conductor-backed coplanar waveguide (CB-CPW). The CB-CPW slot lines and the gap between two metallic via rows play a prominent role in widening the bandwidth and reducing the loss. The CB-CPW-CVWSIW transition is initially designed in the 4-8 GHz (C-band) range. Following the same design procedure, the transitions are made for other five different bands to cover the frequencies from 2 to 40 GHz. Improved performance in terms of bandwidth, insertion loss, and total loss is the benefit of the designed transitions with the proposed CVWSIW. Laboratory prototypes of the transitions are fabricated and experimentally measured to cross verify the simulation results. The measured results show, for example, the minimum return loss of 15 dB, maximum insertion loss of 0.36 dB, and fractional bandwidth of 62.16% for C-band.**

***Index Terms*—Conductor backed-CPW, corrugated via-wall substrate-integrated Waveguide (CVWSIW), Low losses, Broadbanding, High fractional bandwidth.**

I. Introduction

Planar transmission lines (TLs) have been broadly used in radio frequency (RF), microwave, mm-wave, and THz applications such as filters, antennas, and as parts of other active/passive circuits [1], [2]. The wide use of planar TLs is due to their low cost, easy availability, and simple fabrication. Yet, the limited conductivity of the metal traces and substrate dielectric losses prevent them from achieving low insertion losses (IL), high return losses (RL) and wide bandwidth, especially as frequency increases into mm-wave and THz regions [3]. Three-dimensional (3D) waveguides often exhibit a superior performance than that of planar TLs; yet their fabrication cost is significantly higher.

The substrate integrated waveguide (SIW) proposed in 1998 [4] and realized in 2001 [5] produced a structure offering superior performance than planar TL at a much lower cost than 3D waveguides. As planar TLs such as microstrip lines (MLs) and coplanar waveguides (CPWs) are widely used for 2-D circuits implementations, low-loss broadband transitions from these TLs to SIW are required for design of entire systems

The primary reasons for the widespread use of CPWs are their low dispersion and broadband performance. Several

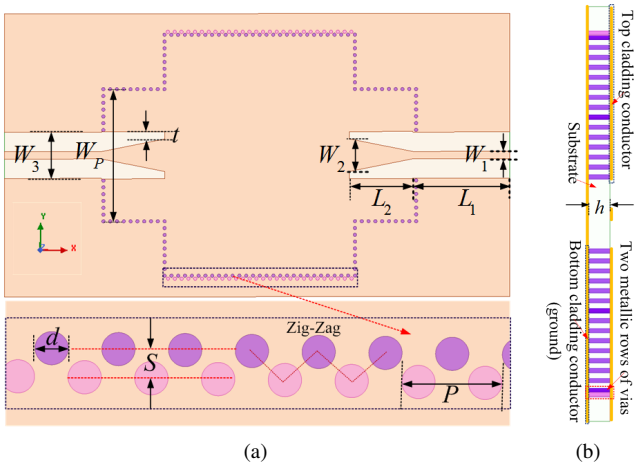

Fig. 1. Proposed CB-CPW to CVWSIW transition: (a) top view (b) cross sectional view.

techniques have been used to design CPW to SIW transitions [6–13]. The first CPW to SIW transition [6] had the aim to make it compatible with LTCC multilayer processes for low-cost production. In [7], a wideband CPW to SIW transition has been designed for mm-wave frequency. A transition from grounded CPW (GCPW) to SIW has been suggested in [8]. UWB transitions, from ML (or its variants like conductor-backed CPW) to SIW, have also been reported [9–12]. Multilayered microstrip to grounded-CPW transitions have been used in the implementation of SIW filter in Ka-band [13]. A low loss and broadband transitions between SIW and rectangular waveguide (RWG) are reported in [14–16]. The IL of 0.5 dB, and fractional bandwidth (FBW) of 6.6% in [14] and IL less than 0.6 dB and 15 dB RL with FBW of 17.34% in [15] have been obtained. All these techniques contributed to the reduction of insertion and increasing return losses, widening of bandwidth, and the transitions size. Some of them were successful in achieving desirable low-loss, low-cost transitions, yet further research is required to enhance the performance of SIWs and the transitions for them.

In this paper, the concept of corrugated via-wall SIW (CVWSIW) initially proposed in [17], [18], and the transition from CB-CPW with this SIW, are studied extensively. It is shown, by extensive simulations that the proposed CVWSIW reduces the IL and enhances the bandwidth of the transitions

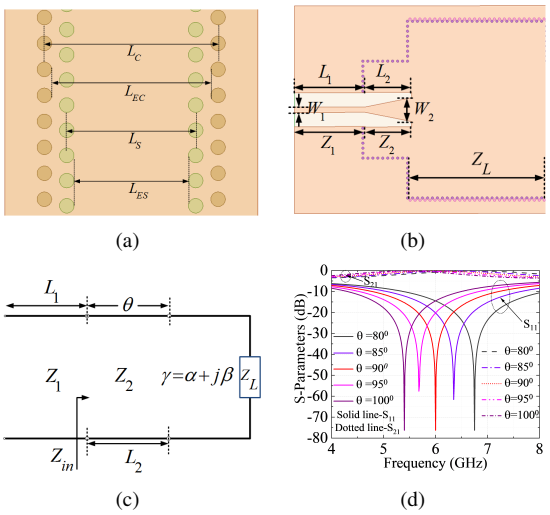

Fig. 2. CB-CPW to CVWSIW transition: (a) top view ($W_3 = 9.6$, $W_P = 23.1$, $L_{ES} = 28.95$, $L_{EC} = 31.30$, $L_S = 29.31$, $L_C = 31.11$, for $C-$ band; unit: *millimetres*), (b) location of electric parameters ($\lambda_g/4$ transformer has impedance Z_2), (c) equivalent electric circuit, (d) electrical length θ and S-parameters of CB-CPW to CVWSIW transition.

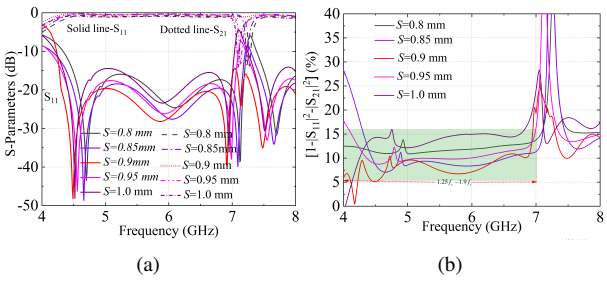

Fig. 3. Effect of S on S-parameters: (a) magnitude of S-parameters and (b) total loss.

Table I
DESIGN DIMENSIONS, THE RETURN LOSS (RL) AND INSERTION LOSS (IL) AT DIFFERENT FREQUENCY BANDS (CB-CPW TO CVWSIW)

Frequency Band / Parameters (mm)	S	C	X	Ku	K	Ka
f_c	1.98	3.70	6.35	9.53	14.30	21.32
P	0.95	0.87	0.83	0.79	0.76	0.7
d	0.60	0.55	0.52	0.5	0.48	0.44
L_S	54.5	29.31	17.21	11.57	7.81	5.32
L_C	57.94	31.11	18.77	12.68	8.61	6.07
S	1.72	0.9	0.78	0.56	0.40	0.38
W_1	1.84	1.82	1.80	1.79	1.76	1.75
L_1	17.55	8.78	5.48	3.95	2.4	1.64
W_2	12.45	7.6	6.7	3.92	2.89	2.54
t	2.5	2.0	1.95	1.83	1.78	1.3
Minimum RL-S*/M* (dB)	15.34/ 14.82	16.38/ 16.94	17.24/ 14.38	12/ 15	17.83/ 17.51	15/ 12.87
Maximum IL-S*/M* (dB)	0.4/ 0.8	0.42/ 0.36	0.86/ 1.05	0.73/ 1.36	1.02/ 1.42	1.04/ 1.48

S*=simulated; **M***=measured

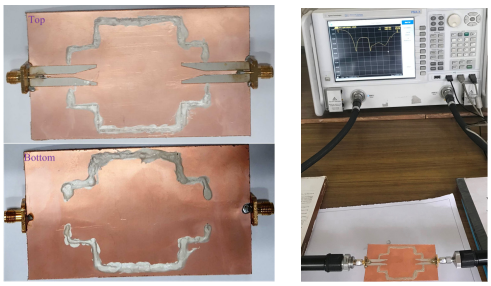

Fig. 4. Laboratory prototypes and measurement setup of the transition: (a) top and bottom views, (b) The back-to-back transitions with VNA.

compared to the previously reported results. First, a prototype of the CB-CPW to CVWSIW transition in 4-8 GHz range was designed, fabricated, and measured. Then five additional CB-CPW to CVWSIW transitions are designed, fabricated, and measured in the 2-40 GHz range. For these additional transitions, the results are represented only by the plots of S_{11} and S_{21} parameters.

II. DESIGN AND WORKING PRINCIPLE OF THE TRANSITION

The transitions from CB-CPW to CVWSIW are designed for S to Ka-frequency ranges. An example given below is designed for C-band (4-8 GHz). The same design approach was extended to other bands (the results for IL and RL are given in Table I).

The proposed transition is shown in Fig. 1 (a) (top view) and Fig. 1 (b) (cross-section view). The main difference of this transition with respect to other TL to CVWSIW transition is that the external wall of vias is extended to the beginning of the quarter-wave transformer. The transition is designed on a single-layer Rogers RT Duroid $588LZ$ substrate having ε_r = 1.96, $\tan\delta$ = 0.0019, and h = 0.508 mm. All the simulations were carried out using the electromagnetic simulator HFSS ver. 2020R2.

The design parameters W_1, L_1, L_2, W_2, W_3, L_{ES}, , d, P, L_{EC}, S, and W_P are shown in Fig. 1 and 2 and dimensions are tabulated in Table I. The C-band cutoff frequency f_c or the fundamental mode (TE_{10}-mode) of the waveguide is calculated as in [19]. At C-band, the estimated range of impedance bandwidth is found as $1.25f_c - 1.9f_c$ at $f_c = 3.7$ GHz. It gives the range from 4.625 GHz to 7.02 GHz. The dimensions, d, P, and L_{ES} are calculated as suggested in [19]. The main design problem is the impedance matching between the feed and tapered section. To set the characteristic impedance of the input line equal to 50 Ω one has to change the width W_1. In order to achieve this, W_1 was fixed at 1.82 mm. The CVWSIW with $\lambda_g/4$ transformer and its equivalent electric diagram is shown in Fig. 2(c).

When Z_{in} (input impedance) = Z_0 (characteristic impedance) is achieved, the transmission line is perfectly matched. The relation between the reflection coefficient (Γ) and standing wave ratio (SWR) with respect to Z_2 was given in [1].

$$Z_{in} = Z_2\left[\frac{1+|\Gamma|}{1-|\Gamma|}\right] = \frac{Z_2}{SWR} = Z_0 \qquad (1)$$

So, the feed line is practically matched with the CVWSIW section if $|\Gamma| = 0$. In fact, when SWR = 1, this condition

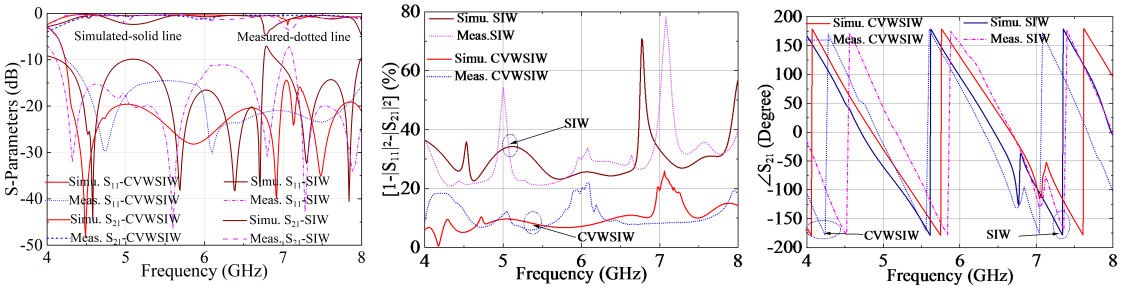

(a) (b) (c)

Fig. 5. Comparison of SIW and CVWSIW transitions: (a) $|S_{11}|$ and $|S_{21}|$, (b) total loss, and (c) phase of S_{21}.

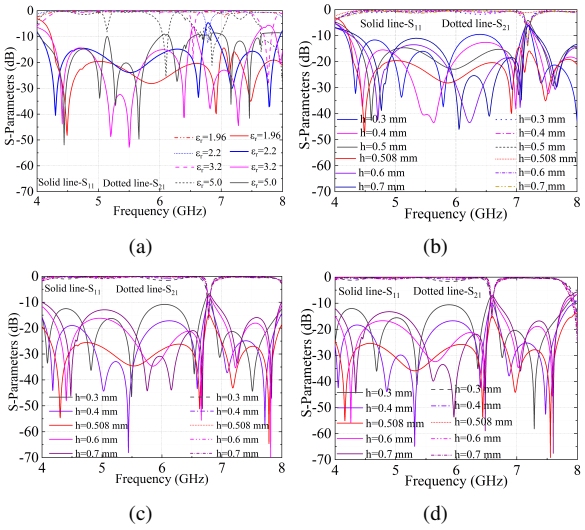

(a) (b) (c) (d)

Fig. 6. Dependence of S_{11} and S_{21} from dielectric constant (ε_r) and thickness (h): (a) variation of ε_r with h = 0.508 mm, (b) variation of h with ε_r = 1.96, (c) variation of h with RT/duroid 5880^{TM} (ε_r=2.2) and (d) variation of h with RT/duroid 5870^{TM} (ε_r=2.33).

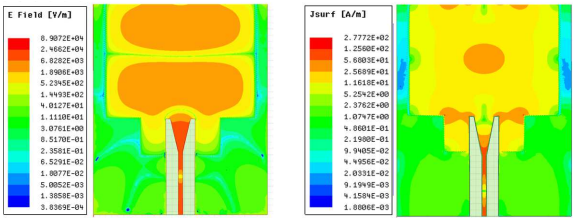

(a) (b)

Fig. 7. Electric and magnetic field patterns in the transition at 6 GHz: (a) electric field (b) magnetic field.

is satisfied if and only if the short circuit condition at the other end of the transition is present. Hence, it is found that $Z_{in} = Z_0$ at $L_2 \approx \frac{\lambda_g}{4}$. To verify this result, RL and IL of transmission line analysis were used. The ADS software has been utilized, and these parameters obtained at 6 GHz are shown in Fig. 2(d). The frequency shift of these parameters with the variation of θ confirms that the change of L_2 is influencing the impedance matching. Finally, $\theta = 90^0$ was used. The important concern of this work was also to reduce the overall losses, and exactly for this we used the CVWSIW technique. The gap S between two metallic rows (Fig. 1(a)) plays a significant role in decreasing these losses. The final dimension of the gap was set after the detailed simulations as, described below.

The influence of S on S-parameters and the total loss is shown in Fig. 3. When S increases from 0.8 to 1.0 mm with the step size of 0.05 mm, the S_{11}-parameter is also improving (Fig. 3 (a)), and at S = 0.9 mm this parameter has a surge. This resulted in fixing S at 0.9 mm. The variation of total loss with respect to S is shown in Fig. 3(b). The minimum total loss of 20% is observed in the entire pass-band at S = 0.9 mm as well.

Fig. 4(a) shows the top and bottom views of the fabricated prototypes, and the measurement setup of back-to-back transitions is shown in Fig. 4(b). Fig. 5 gives the comparison of the simulated and measured results for CB-CPW to SIW (specially designed for the purpose of comparison) and CVWSIW transitions. The simulated and measured results of the RL and IL are presented in Fig. 5(a). The degraded performance of simulated RL below 15 dB and IL above 1.96 dB are found in the frequency range from 7.0 to 7.1 GHz only. However, the required conditions are satisfied in $1.25f_c - 1.90f_c$ (4.625 to 7.02 GHz) band with $f_c = 3.7$ GHz. Moreover, the measured RL above 16.94 dB and IL below 0.36 dB are achieved in the whole passband. The experimental validation of the overall losses in both SIW and CVWSIW cases is shown in Fig. 5(b). It is observed that the total loss of CVWSIW is lesser than that of SIW transition, although an average absolute loss difference between CVWSIW and SIW transitions is approximately 20.0%. The comparison of S_{21} phase variation is given in Fig. 5(c), and an early change in the phase for CVWSIW case marks the reduced loss in design.

For the CVWSIW, the distance between two rows of metallic vias (S) varies from $0.0289L_C$ to $0.0717L_S$ range. The tapered width is fixed by using parametric analysis at the individual frequency range, as mentioned in Table I. The length of the tapered part can be set by choosing.

$$L_2 = 0.2457\lambda_g \tag{2}$$

The gap t (Fig. 2(a)) between the feed and ground can be fixed in $0.035\lambda_g - 0.1937\lambda_g$ range (this is the same as changing W_2).

The transition was made using the material with dielectric constant ε_r of 1.96 and the thickness h of 0.508 mm. Yet, additional simulations were done to evaluate the influence of

these two parameters on the transition properties. The results are presented in Fig. 6. Fig. 6(a) shows the simulated S-parameters for h = 0.508 mm and four different values of ε_r (1.96, 2.2, 3.2 and 5). It is observed that the RL above 15 dB, and IL below 1.96 dB are in all cases except of ε_r = 5.0. In case of ε_r=5.0, the RL is above 8.29 dB only and IL is more than 3 dB (even though in some points only) in the specified band. Fig. 6(b) shows the parameters when the substrate thickness changes from 0.3 to 0.7 mm with the step of 0.1 mm. Fig. 6(b) where ε_r = 1.96 shows that RL and IL become critical when h = 0.6 and 0.7 mm, whereas for other values of h, they have satisfactory values acceptable for transition design, i.e., the reflection loss is above 15 dB and the insertion loss is below 1.96 dB. The simulated RL and IL for other values of ε_r (2.2 and 3.2,), and the same variation of h (in mm: 0.3, 0.4, 0.5, 0.6, and 0.7), for each value of the mentioned ε_r, are presented in Fig. 6(c)-(d), respectively.

The electric and magnetic field patterns at 6 GHz for the designed transition are shown in Fig. 7(a) and (b). The confinement of the fields inside the waveguide is clearly seen.

III. Experimental Validation and Discussion

The successful design, simulation, and experimental verification of the CB-CPW to CVWSIW transition for the C-band frequency range allowed us to expand the approach to other frequency bands as well (Table I). It was extended for the frequencies of 2-40 GHz (S-Ka bands) range. The simulated and measured results of the S-parameters for these transitions are shown in Fig. 8(a)-(e). It can be observed that the simulated and measured RL and IL are closely matched in all bands. The measured reflection coefficient is below 16.94 dB (16.38 dB simulated) and insertion loss is below 0.36 dB (0.42 dB simulated) in the entire pass-band for all frequency bands. In some cases, the empty vias in the PCB were manually filled with copper paste, and this resulted in a higher IL for these designs in comparison with simulated results. Moreover, the length of SIW is 24 mm, whereas the overall length of the structure is 104 mm. The measured IL of 0.36 dB is obtained at 6 GHz, including a total of 6.15 mm 50-Ohm feeding lines for probe measurement consideration. It means the IL is about 0.012 dB/mm at 6 GHz. For measurements (ML, CB-CPW to CVWSIW transitions), an electronics calibration (Ecal, VNA No.: Agilent N5247A (10 MHz-67 GHz)) is used to de-embed the influences of the test fixture and its coaxial or SMA connectors. The SOLT (short–open-load-through) calibration is also used in order to cross-verify with E-cal.

The comparison of the previously published results on CPW to SIW transitions with the results of the present work is given in Table II. The RL (15 dB) and FBW of the proposed transitions are better than that reported in [8], [10], [11], [13–15]. The IL is lesser than that reported in [8], [11], [13–15] and slightly higher than that reported in [10] (use also Table I). Table II also shows the impedance bandwidth and compares it with the previous work. This result indicates the larger bandwidth in different frequency ranges. We also calculated the total loss for the C-band and found that its level is low. In summary, the proposed transitions exhibit a wider bandwidth, allow an easy fabrication, and may be used as low loss mm-wave component.

Table II
Comparison of Competitive Broadband Transition Designs between CB-CPW and SIWs

References	Frequency range (GHz)	RL (dB)	IL (dB)	Type	BW (GHz/%)
[8]	26-32	≥ 20	≤ 0.73	GCPW	2.84/10
[11]	19-40	≥ 10	≤ 0.9	ECPW	21/70
[13]	20-47	≥ 12	≤ 3.1	GCPW	2/5.92
[14]	32.6-38.1	≥ 15	$\leq 1.2(0.6^*)$	RW-SIW	5.5/17.34
[15]	24-28	≥ 15	≤ 0.5	RW-SIW	1.72/6.6
[10]	2-4	≥ 15	≤ 0.2	CPW	1.35/36.8
This work	**4-8**	$\geq$ **15**	$\leq$ **0.36**	**CB-CPW**	**3.73/62.16**

*=IL for single transition

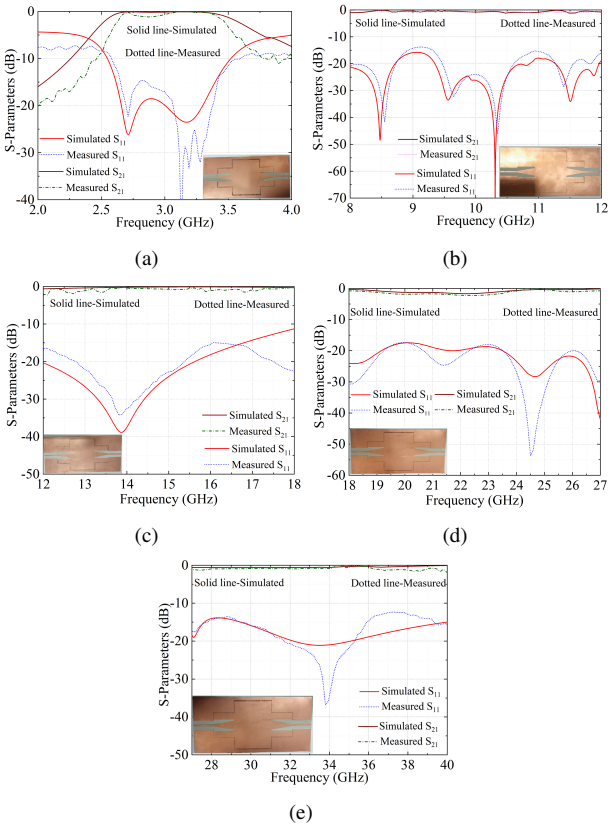

Fig. 8. S_{11} and S_{21} parameters for different frequency bands: (a) *S*-band, (b) *X*-band, (c) *Ku*-band, (d) *K*-band, and (e) *Ka*-band.

IV. Conclusion

We proposed the concept of corrugated via-wall SIW and experimentally verified its improved performance compared to the traditional SIW. The transitions for this CVWSIW with CB-CPW were designed, simulated, and verified experimentally. The proposed CVWSIW and the designed transitions will be helpful in the implementation of compact, low-loss planar circuits and systems for microwave and mm-wave systems.

REFERENCES

[1] D. M. Pozar, *Microwave Engineering, 3rd ed*. New York: Wiley, 2005.

[2] X. H. Wu and A. Kishk, *Analysis and Design of Substrate Integrated Waveguide Using Efficient 2D Hybrid Method, 1st ed.* New York: Morgan & Claypool, 2010.

[3] K. Wu, M. Bozzi, and N. J. G. Fonseca, "Substrate integrated transmission lines: Review and applications," *IEEE Journal of Microwaves*, vol. 1, no. 1, pp. 345–363, 2021.

[4] A. Tugulea and I. R. Ciric, "Two-dimensional equations for microwave planar circuits," in *1998 Symposium on Antenna Technology and Applied Electromagnetics*, Aug 1998, pp. 315–318.

[5] D. Deslandes and K. Wu, "Integrated microstrip and rectangular waveguide in planar form," *IEEE Microwave and Wireless Components Letters*, vol. 11, no. 2, pp. 68–70, Feb 2001.

[6] D. Deslandes and Ke Wu, "Integrated transition of coplanar to rectangular waveguides," in *2001 IEEE MTT-S International Microwave Sympsoium Digest (Cat. No.01CH37157)*, vol. 2, May 2001, pp. 619–622 vol.2.

[7] A. Patrovsky, M. Daigle, and Ke Wu, "Millimeter-wave wideband transition from cpw to substrate integrated waveguide on electrically thick high-permittivity substrates," in *2007 European Microwave Conference*, Oct 2007, pp. 138–141.

[8] D. Deslandes and Ke Wu, "Analysis and design of current probe transition from grounded coplanar to substrate integrated rectangular waveguides," *IEEE Transactions on Microwave Theory and Techniques*, vol. 53, no. 8, pp. 2487–2494, Aug 2005.

[9] Young-Gon Kim, Kang Wook Kim, and Young-Ki Cho, "An ultra-wideband microstrip-to-cpw transition," in *2008 IEEE MTT-S International Microwave Symposium Digest*, June 2008, pp. 1079–1082.

[10] R. Fang, C. Liu, and C. Wang, "Compact and broadband cb-cpw-to-siw transition using stepped-impedance resonator with 90°-bent slot," *IEEE Transactions on Components, Packaging and Manufacturing Technology*, vol. 3, no. 2, pp. 247–252, 2013.

[11] S. Lee, S. Jung, and H. Lee, "Ultra-wideband cpw-to-substrate integrated waveguide transition using an elevated-cpw section," *IEEE Microwave and Wireless Components Letters*, vol. 18, no. 11, pp. 746–748, Nov 2008.

[12] X. Chen and K. Wu, "Low-loss ultra-wideband transition between conductor-backed coplanar waveguide and substrate integrated waveguide," in *2009 IEEE MTT-S International Microwave Symposium Digest*, June 2009, pp. 349–352.

[13] G. Lee, B. Lee, J. Jeong, and J. Lee, "Ka-band surface-mount cross-coupled siw filter with multi-layered microstrip-to-gcpw transition," *IEEE Access*, vol. 7, pp. 66 453–66 462, May 2019.

[14] G. Zhang, H. Yi, S. Wang, and M. Han, "Broadband right-angle transition from substrate integrated waveguide to rectangular waveguide," *Electronics Letters*, vol. 53, no. 7, pp. 473–475(2), 2017.

[15] R. Glogowski, J.-F. Zurcher, C. Peixeiro, and J. Mosig, "Broadband ka-band rectangular waveguide to substrate integrated waveguide transition," *Electronics Letters*, vol. 49, no. 9, pp. 602–604, 2013.

[16] K. Zhu, Y. Xiao, W. Tan, H. Luo, and H. Sun, "A broadband e-band single-layer-siw-to-waveguide transition for automotive radar," *IEEE Microwave and Wireless Components Letters*, vol. 32, no. 6, pp. 523–526, 2022.

[17] A. K. Nayak and A. Patnaik, "Design of an siw corrugated h-plane horn antenna with improved performance," in *2017 IEEE Applied Electromagnetics Conference (AEMC)*, 2017, pp. 1–2.

[18] A. K. Nayak, V. Singh Yadav, and A. Patnaik, "Wideband transition from tapered microstrip to corrugated siw," in *2019 IEEE MTT-S International Microwave and RF Conference (IMARC)*, 2019, pp. 1–4.

[19] A. K. Nayak, I. M. Filanovsky, K. Moez, and A. Patnaik, "Broadband conductor backed-cpw with substrate-integrated coaxial line to siw transition for c-band," *IEEE Transactions on Circuits and Systems II: Express Briefs*, vol. 69, no. 5, pp. 2488–2492, 2022.